The Stirred Tank Reactor Polymer Electrolyte Membrane Fuel Cell

Jay Benziger, E. Chia, E. Karnas, J. Moxley, C. Teuscher, and I. G. Kevrekidis
Dept. of Chemical Engineering Princeton University, Princeton, NJ 08544

DOI 10.1002/aic.10158
Published online in Wiley InterScience (www.interscience.wiley.com).

The design and operation of a differential polymer electrolyte membrane (PEM) fuel cell is described. The fuel cell design is based on coupled stirred tank reactors (STRs) coupled through a membrane; the gas phase in each reactor compartment is well mixed. The characteristic times for reactant flow, gas phase diffusion, and reaction were chosen so that the gas compositions at both the anode and cathode are uniform. The STR PEM fuel cell is one-dimensional; the only spatial gradients are transverse to the membrane. The cell is used to examine start-up, and dynamic responses to changes in load, temperature, and reactant flow rates. Multiple time scales in the system's response are found to correspond to water absorption by the membrane, water transport through the membrane, and stress-related mechanical changes of the membrane. © 2004 American Institute of Chemical Engineers *AIChE J,* 50: 1889–1900, 2004
Keywords: coupled stirred tank reactor, polymer electrolyte membrane fuel cell, diffusion

Introduction

Fuel cells are multiphase chemical reactors in which two sequential chemical reactions are coupled by transport of the intermediate products between catalysts. The reactants are fed on two sides of the reactor, separated by an ion-conducting barrier. A catalytic reaction occurs on one side of the barrier, producing an intermediate product that is transported across the barrier to a second catalyst, where it reacts with the second reactant to make the final product. A simplified version of the polymer electrolyte membrane (PEM) fuel cell is shown in Figure 1 (Blomen and Mugerwa, 1993; Bokris and Srinivasan, 1969; Costamagna and Srinivasan, 2001; EG&G Services, 2000). Hydrogen molecules are fed to the anode side of a cation-conducting polymer membrane in contact with a catalyst. The hydrogen molecules react on the anode catalyst, producing the intermediate products: protons and electrons. The protons are transported across the PEM and the electrons pass through an external circuit, where they encounter oxygen molecules on the cathode side of the membrane. The protons, electrons, and oxygen react on the cathode catalyst surface and produce water.

A reaction engineering approach to analyze PEM fuel cells is introduced. We are seeking a *prescriptive* model of the PEM fuel cell, which describes the system response as a function of the parameters that the operator can control. The experimental approach is based on experience with heterogeneous catalytic reactors. Experimental results from simplified reactors are used to develop mathematical descriptions of the system variables as functions of the system operating parameters that fit the data over the relevant range of operating conditions (Froment and Bischoff, 1979). Model reactors, such as the one described herein, are not optimal for reactant conversion; rather, they are specifically designed to measure system parameters, including effective kinetic and transport properties (Folger, 1999; Froment and Bischoff, 1979; Levenspiel, 1996).

There are a number of excellent models of the transport processes and the detailed chemical reactions at the electrocatalyst surfaces in PEM fuel cells (Baschuk and Li, 2000; Bernardi, 1990; Bernardi and Verbrugge, 1992; Dutta et al., 2000; Natarajan and Van Nguyen, 2001; Springer et al., 1991, 2001; Thampan et al., 2000; Van Nguyen and Knobbe, 2003). These models have included molecular details of electron transfer reactions at electrode surfaces, transport of the reac-

Correspondence concerning this article should be addressed to J. Benziger at benziger@princeton.edu.

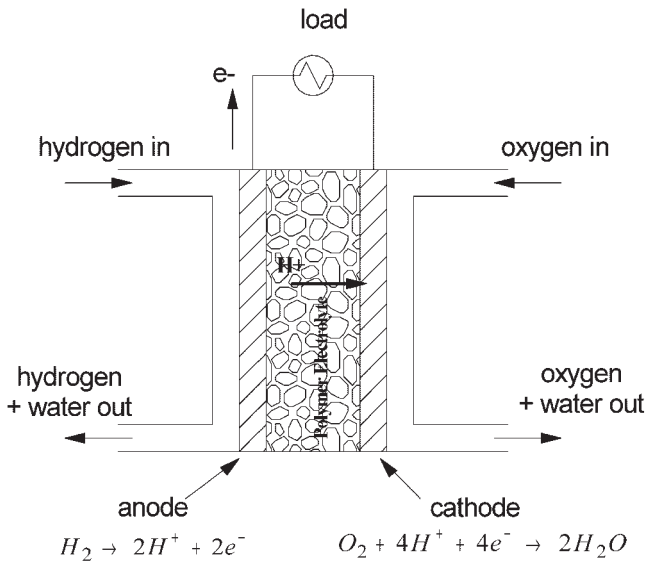

Figure 1. Hydrogen-oxygen PEM fuel cell.

Hydrogen molecules dissociatively adsorb at the anode and are oxidized to protons. Electrons travel through an external load resistance. Protons diffuse through the PEM under an electrochemical gradient to the cathode. Oxygen molecules adsorb at the cathode, are reduced, and react with the protons to produce water. The product water is absorbed into the PEM, or evaporates into the gas streams at the anode and cathode.

tants and products through multiple layers associated with the electrodes, and transport of water and protons through the polymer electrolyte. Steady-state current/voltage response characteristics of a PEM fuel cell have been successfully fit by these models. However, these models are complex and they have not been validated with *dynamic* behavior of PEM fuel cells. Indeed, these models have emphasized steady-state performance.

We designed and constructed an "idealized" experimental fuel cell to examine fuel cell dynamics. Herein we describe the stirred tank reactor (STR) PEM fuel cell and the rationale behind its design. The STR PEM fuel cell is compared to existing fuel cell test stations to illustrate its unique features and capabilities. A systems analysis is presented to identify the key control parameters affecting the operation of PEM fuel cells. A reaction engineering model of a differential element in a PEM fuel cell is presented to show the essential information required to predict dynamic behavior. Finally, we present results of the startup of PEM fuel cells and their response to changes in load, temperature, and reactant flow.

The Differential PEM Reactor

The STR PEM design

Our STR PEM fuel cell is shown in Figure 2A. The membrane–electrode assembly (MEA) was pressed between two machined graphite plates and sealed with a silicon rubber gasket. Gas plenums of volume $V \sim 0.2$ cm^3 were machined in graphite plates above a membrane area of about 1 cm^2. There were several pillars matched between the two plates to apply uniform pressure to the MEA. Hydrogen and oxygen were supplied from commercial cylinders (Airco) through mass flow controllers at flow rates $Q \sim$ 1–10 cm^3/min (mL/min). The residence times of the reactants in the gas plenums ($V/Q \sim$ 1.2–12 s) were greater than the characteristic diffusion time ($V^{2/3}/D \sim$ 0.3–1 s), ensuring uniformity of the gas compositions. The cell temperature was controlled by placing the graphite plates between aluminum plates fitted with cartridge heaters connected to a temperature controller. The entire fuel cell assembly was mounted inside an aluminum box to maintain better temperature uniformity (see Figure 2b).

Gas pressure was maintained in the cell by placing spring-loaded pressure relief valves (Swagelok) at the outlets. Tees were placed in the outlet lines (inside the aluminum box) with relative-humidity sensors in the dead legs of the tees. The water content of the outlet streams was measured with humidity sensors (Honeywell HIH 3610), and the temperature at the

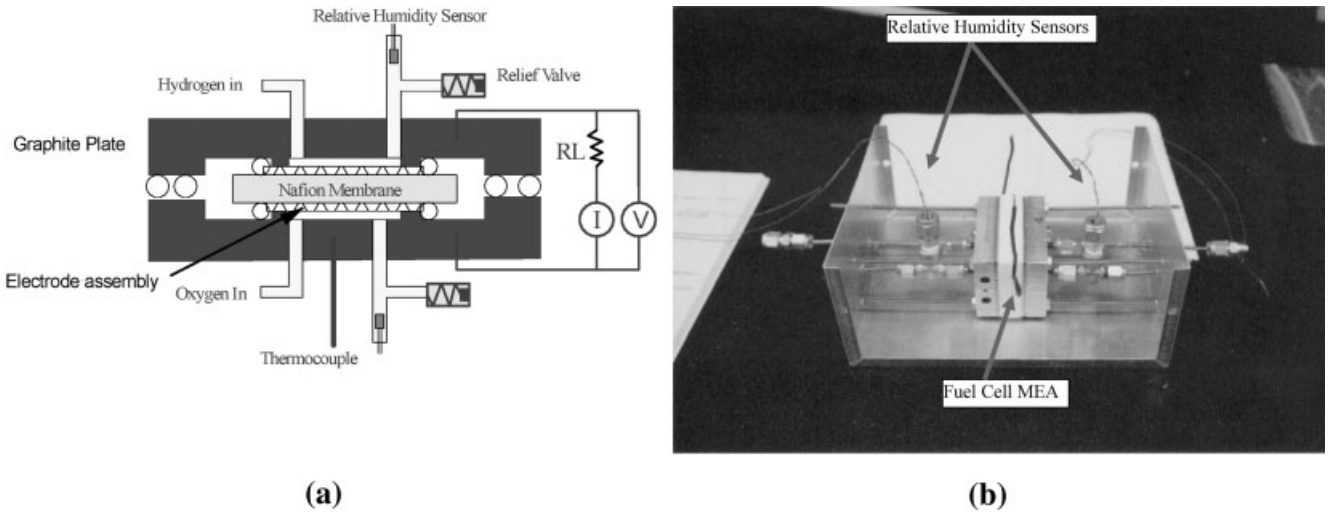

Figure 2. STR PEM fuel cell.

(a) The exposed electrode area was about 1 cm^2 on each side, with gas volumes above the anode and cathode of about 0.2 cm^3. The MEA used E-tek electrodes and a Nafion 115 membrane. (b) The graphite plates were fitted into Teflon plates and sandwiched between heated Al blocks. Relative humidity sensors measured the temperature and RH in the effluent streams.

humidity sensor was measured with a thermocouple in the gas line. The relative-humidity sensors had to be sufficiently heated to avoid liquid condensation on the capacitive sensing element, but they also had to be kept below 85°C to protect the amplifier circuit on the sensor chip.

Any suitable MEA can be tested in the STR PEM fuel cell. We report here results using an MEA consisting of a Nafion 115 membrane pressed between 2 E-tek electrodes (these consist of a carbon cloth coated on one side with a Pt/C catalyst). The catalyst weight loading was 0.4 mg Pt/cm^2. The electrodes were brushed with solubilized Nafion solution to a loading of about 4 mg Nafion/cm^2 before placing the membrane between them (Raistrick, 1989). The assembly was hot pressed at 130°C and 10 MPa. Copper foils were pressed against the graphite plates and copper wires were attached to connect to the external load resistor.

The current and voltage across the load resistor were measured as the load resistance was varied. A 10-turn 0–20 Ω potentiometer was connected in series with a 10-turn 0–500 Ω potentiometer. The load resistance was varied from 0 to 20 Ω to obtain a polarization curve (*IV*). To examine the low-current range of the polarization curve the resistance had to be increased over the range of 0–500 Ω. The voltage across the load resistor was read directly by a DAQ board. The current through the load resistor was passed through a 0.2-Ω sensing resistor and the differential voltage across the sensing resistor was amplified by a factor of 100 with an Analog Devices AMP02 Instrumentation Amplifier and read by the DAQ board. An *IV* curve was typically collected and stored in about 100 s.

Comparison of the STR PEM and serpentine flow PEM test stations

The fundamental difference between our STR PEM fuel cell reactor and the standard PEM fuel cell test station is associated with the gas flow fields. Figure 3 compares the serpentine flow fields for a GlobeTech Fuel Cell Test Station 2 and our STR PEM fuel cell reactor. The GlobeTech test station has an MEA area of 5 cm^2, with serpentine flow channels approximately 100 mm long and 1 mm^2 cross-sectional area. In the STR PEM the MEA area is about 1 cm^2 and flow channels are approximately 14 mm long with a cross-sectional area of 4 mm^2. Mixing in the gas flow channels is characterized by the ratio of diffusive transport (D/L = diffusivity/length of flow channel) to convective transport (u = gas velocity). When $D/uL > 1$ diffusive mixing dominates over convective flow and there will be homogeneity in the fluid composition.

The characteristic dispersion number at both the anode and cathode is ≥ 1 when the feed flow rates to the STR PEM <10 cm^3/min (corresponding to a current density of 1.4 A/cm^2 at 100% hydrogen utilization). In contrast, the dispersion number is <0.02 for the serpentine flow channels with flow rates of 50 cm^3/min (also corresponding to an average current density of 1.4 A/cm^2 at 100% hydrogen utilization). Diffusive mixing in the STR PEM homogenizes the gas-phase composition at each electrode. However, convection in the serpentine flow PEM fuel cell test station results in compositional variations along the length of the flow channels. In terms of idealized chemical reactors, the GlobeTech test station is a *plug flow reactor*, whereas our differential reactor is a *stirred tank reactor*. The gas-phase uniformity above the anode and cathode simplifies the analysis of the STR PEM data. The system is one dimensional (1-D); only gradients transverse to the membrane are important. The current density, or reaction rate, in the STR PEM fuel cell is also spatially uniform; at steady state the reaction rate is equal to the difference between the molar flows of the feed and effluent.

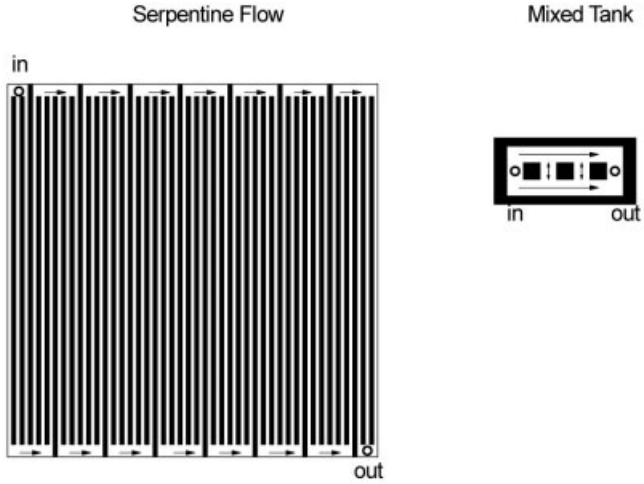

Figure 3. The flow fields, machined in graphite plates, for a "typical" (GlobeTech) PEM test station and for the STR PEM reactor.

The Serpentine flow channels cover an area of 5 cm^2, whereas the STR PEM fuel cell covers an area of about 1 cm^2. The two different configurations are drawn to the same scale. The open plenum area of the STR PEM reactor permits sufficient diffusive mixing to give near uniform gas-phase composition. The dark areas are raised and contact the membrane–electrode assembly.

It is possible to operate the serpentine flow channel test station in a differential mode by limiting the reactant conversion so the concentration gradients *along the flow channel* are small. Keeping the fractional conversion of the reactants $<5\%$ will give nearly homogeneous compositions at the anode and cathode. However, the current density should be limited to 60 mA/cm^2 for a serpentine flow channel test station to be differential.

System analysis of PEM fuel cells

The greatest utility of the STR PEM fuel cell reactor is to isolate and focus on the features of the dynamics of PEM fuel cells. Specific questions to be explored are as follows:

(1) How long does it take a PEM fuel cell to start up from different initial conditions? How do the system parameters affect start-up of the fuel cell?

(2) How does the PEM fuel cell respond dynamically to changes in load? Temperature? Gas flow rate?

(3) How should the system parameters be controlled under conditions of variable load, such as those encountered in automotive applications?

Our objective in this report is to demonstrate the experimental concept of a 1-D PEM fuel cell. Although there are numerous 1-D models of PEM fuel cells in the literature, there are no reports of a 1-D experimental system. The results presented herein highlight some of the complexities associated with PEM

Table 1. System Variables and System Parameters for a PEM Fuel Cell

System Variables	System Parameters
Reactant flow rates	Reactant feed flow rates
Reactant composition	Reactant feed composition
Gas relative humidity	Heat input
Cell temperature	External load resistance
Cell voltage	Electrode composition and structure
Cell current	Membrane material
Membrane water content/resistance	Cell construction

fuel cell dynamics we have identified with our STR PEM fuel cell.

A real PEM fuel cell reactor is complex. Electrode reactions and transport through the gas channels, diffusion through the electrode layers, and transport across the membrane are all coupled. Datta and coworkers described the structure of PEM fuel cells and the molecular details of the transport and reaction in the PEM fuel cell (Thampan et al., 2001). These models assume descriptions about transport processes and electrode kinetics and call for data about system variables that cannot be directly measured or easily controlled. We have followed an engineering approach and considered to what level of detail the system variables in the fuel cell can be described as functions of the parameters under operator control. Our ultimate objective is to develop a good reactor model that captures the essential physics without unnecessary detail.

Table 1 summarizes the system variables and system parameters for a PEM fuel cell. The system parameters are under operator control, whereas the system variables describe the local state of the PEM fuel cell. For example, the feed to the fuel cell can be regulated, but the local composition and flow rate along the flow channel are determined by dynamic mass balances. Similarly, water supplied in the feeds is a controlled parameter, whereas the local membrane water content is a system variable that depends on the balance between water supplied in the feed, water produced at the cathode, and water removed in the effluents. The fuel cell current and voltage are *system variables* determined by the state of the membrane and the entire circuit including the controllable external load resistance. We will report operation of the STR PEM reactor under conditions of defined load resistance—not galvanostatically or potentiostatically controlled.

We can divide the system parameters listed in Table 1 into two groups. One group of parameters is fixed by the choice of reactor construction, and those remain fixed unless one builds a new reactor. These parameters include choice of membrane, catalyst, and flow field. The second group consists of the parameters that can be manipulated externally during the operation of the fuel cell reactor. These are the feed flow rates, the feed compositions, the heat input (or removal), and the external load resistance. Ideally one would like to know the values of all the system variables during the fuel cell operation. In practice only a few of these quantities are directly observable (measurable). We have designed our STR PEM fuel cell so that the temperature, pressure, gas-phase water content in the anode and cathode effluents, and the cell current and voltage can be measured. The STR PEM fuel cell minimizes lateral spatial variations, so the current density and gas composition are uniform across the gas–electrode–membrane interface.

The STR PEM fuel cell can be thought of as a differential element along the flow channel in a PEM fuel cell. The differential element is shown in Figure 4A, along with the differential material balances. Our STR PEM fuel cell is small and generates little heat. It is surrounded with a large heat source/sink creating a uniform temperature. Under these conditions temperature may be treated as a fixed system variable. We use a lumped parameter model (Figure 4B), which emphasizes the functional description of the fuel cell based on controllable parameters and observable variables. Equations 1–9 summarize the model equations in the differential reactor element. Equations 1–3 are mass balances for hydrogen, oxygen, and water. Equation 7 represents the reaction rate for water formation, which is equal to 1/2 the proton current. The remaining equations are the relations between different system variables. The terms in the equations are defined later in the notation section.

Reactor model of a PEM fuel cell

The system parameters for the fuel cell are slightly different from those of a typical chemical reactor. In addition to feed flow rates, composition, and temperature, the external load resistance is a new parameter. The fuel cell can be thought of as a set of reactors connected through a set of flow regulators, as shown in Figure 5. Hydrogen molecules are oxidized to protons and electrons at the anode. The resistances in the membrane and external load regulate the current in the fuel cell (that is, the flow of protons and electrons). The protons and electrons meet up at the cathode along with the oxygen to produce water. The external load resistance is analogous to a valve that regulates the flow of product out of the anode reactor to the cathode reactor.

The coupling of reactor elements shown in Figure 5 is the basis for our analysis of the fuel cell as a chemical reactor. The system parameters are the feed flow rates, composition, the heat input, and the external load resistance. We present data with the external load resistance as the independent parameter. This is different from the traditional electrochemistry approach, in which PEM fuel cells are operated under galvanostatic or potentiostatic control (constant current or constant voltage). When the chemical reaction is driven by the imposition of an external electrical driving force, such as with electrolysis of water, the current or voltage is a system parameter that can be independently manipulated. However, in a fuel cell the chemical reaction drives the current through the external load, and the load resistance is the system parameter that can be manipulated. Constant current or voltage requires a feedback controller that adjusts the external resistance to maintain the current or voltage. We seek to understand the *autonomous* operation of the PEM fuel cell; operation of the fuel cell under galvanostatic or potentiostatic control distorts the autonomous dynamics and obscures the direct determination of kinetics.

In the STR PEM fuel cell we set the feed conditions, the temperature, and the external load resistance. We measure the effluent flow rate and composition, the voltage across the external load, and the current through the external load. The key system variable that we cannot measure directly in our setup is the *membrane water activity*. The membrane water activity determines the proton conductivity of the membrane, which along with the external load resistance controls the

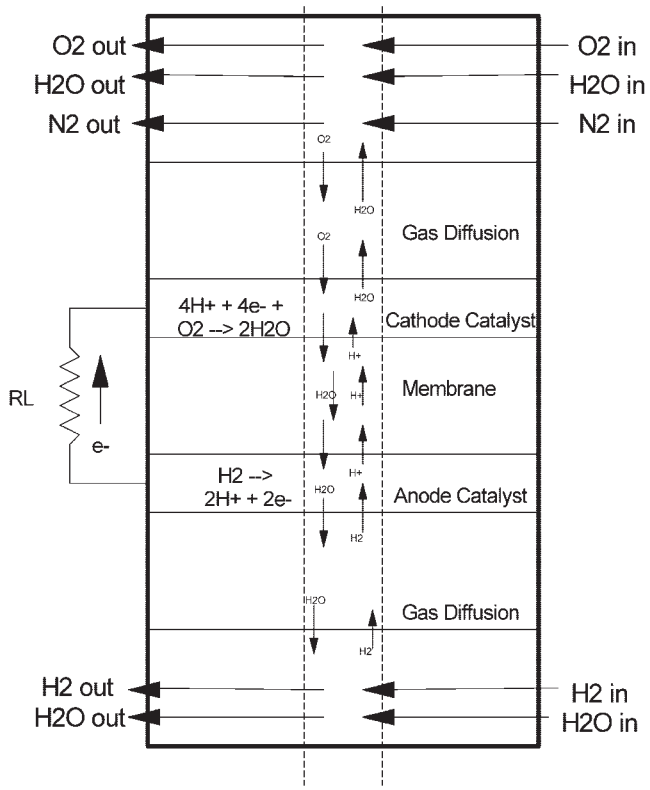

Figure 4a. Reaction and diffusion processes in a differential element in a PEM fuel cell.

The detailed transport processes through the multiple layers of the membrane–electrode assembly are illustrated. The flows entering the differential element from the right and the load resistance on the left are the controllable system parameters.

$$\frac{V_A}{RT}\frac{\partial P_{H_2}^{out}}{\partial t} = \left(\frac{Q_A^{in}P_{H_2}^{in}}{RT} - \frac{Q_A^{out}P_{H_2}^{out}}{RT}\right) - \frac{i}{2F} \quad (1)$$

$$\frac{V_C}{RT}\frac{\partial P_{O_2}^{out}}{\partial t} = \left(\frac{Q_C^{in}P_{O_2}^{in}}{RT} - \frac{Q_C^{out}P_{O_2}^{out}}{RT}\right) - \frac{i}{4F} \quad (2)$$

$$\frac{\partial N_w^m}{\partial t} = \left(\frac{Q_A^{in}P_w^{A,in}}{RT} - \frac{Q_A^{out}P_w^{A,out}}{RT}\right) + \left(\frac{Q_C^{in}P_w^{C,in}}{RT} - \frac{Q_C^{out}P_w^{C,out}}{RT}\right) + \frac{i}{2F} \quad (3)$$

$$N_w^m = \frac{\rho_m A_m(\Delta z)}{EW}\lambda_w \quad (4)$$

$$\lambda_w = f(a_w^m, T) \quad (5)$$

$$a_w^m = f(a_w^A, a_w^C) \quad (6)$$

$$i = \frac{V_{eff}}{R_L + R_m} \quad (7)$$

$$R_m = f(a_w^m, T) \quad (8)$$

$$V_{eff} = -\frac{\Delta G^o}{4F} + \frac{RT}{4F}\ln\left(\frac{P_{H_2}^2 P_{O_2}}{P_{H_2O}^2}\right) - \eta(a_w^m, R_L) \quad (9)$$

Figure 4b. A lumped parameter scheme was used for the model equations.

The scheme is expressed in controllable parameters [inlet flow rates (Q_i), inlet compositions (P_i), and the external load resistance (R_L)] and observable system variables (voltage, current, local composition, membrane water activity).

current and voltage associated with the fuel cell. Equation 9 relates the effective fuel cell voltage to the system variables and parameters; the first two terms on the right-hand side of Eq. 9 are the thermodynamic potential. The last term is the overpotential, representing a kinetic limitation. We have expressed the overpotential as a function of water activity in the membrane and load resistance. Normally the overpotential is expressed as a function of the current density. However, the load resistance and membrane resistance, which is a function of the water activity, determine the current and in turn the overpotential.

Dynamic Operation of the STR PEM Fuel Cell

A PEM fuel cell must have sufficient water content for the fuel cell to function; but how much water is sufficient? We show two experiments that illustrate the importance of water in the start-up of PEM fuel cells. A series of experiments are then presented where changes in the system parameters alter the balance between water production and removal and change the water activity in the membrane. The membrane is a reservoir for water, and the resistance of the membrane changes as the water inventory changes. The coupling the electrical resistance and the water content results in a feedback loop that can cause complex dynamics in the PEM fuel cell.

Startup of the autohumidification STR PEM fuel cell

Autohumidification refers to fuel cell operation with dry feed gases; the water to humidify the membrane is produced by the fuel cell reaction. Shown in Figure 6a is the current response for start-up of the STR PEM fuel cell operated in the autohumidification mode. Before start-up of the STR PEM fuel cell, the initial water content in the membrane and the load resistance were fixed. The polymer membrane was dried by flowing dry oxygen through the cathode chamber at about 100 mL/min and dry nitrogen through the anode chamber at about 100 mL/min for about 12 h at 60°C. To humidify the membrane, the oxygen flow was shut off, and 10 mL/min nitrogen flow was passed through a water bubbler at room temperature and into the anode chamber. The relative humidity was measured at the outlet of the anode as a function of time, to determine the water

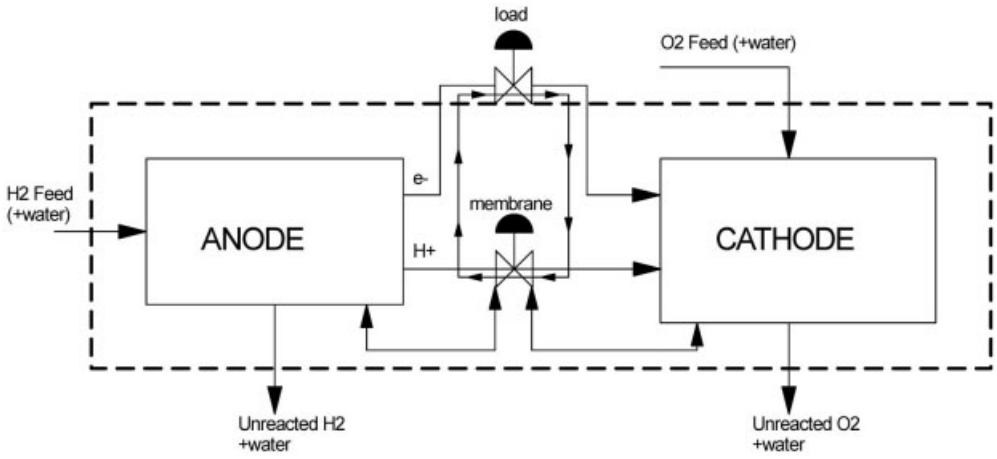

Figure 5. Conceptual reactor coupling in a fuel cell.

The heavy dashed line represents the physical boundary of the fuel cell. The feed flow and composition at the anode and cathode are system parameters shown as inputs. The effluents leaving the anode and cathode are system variables. The membrane and the external load resistance for the fuel cell are analogous to valves that regulate flow of the intermediate products from the anode to the cathode. The dashed line going through the valves indicates that the resistance to flow of those two regulating valves is in series. The load resistance is shown external to the fuel cell boundary because it is a system parameter. Water is shown moving between the cathode and anode through the membrane. The water flux depends on the concentration gradients and the current (by electro-osmotic drag).

uptake by the membrane. After hydrating the membrane to the desired level, the nitrogen flow was stopped. Hydrogen flow at 10 mL/min to the anode and oxygen flow at 10 mL/min to the cathode were initiated, and the current through the load resistor (set at 5 Ω) was measured as a function of time. For initial membrane water concentrations of <0.6 mg/cm^2 the fuel cell current decayed with time to near zero (the fuel cell current was "extinguished"). When the initial water concentration in the membrane was about 0.8 mg/cm^2 the fuel cell current "ignited," increasing from an initial value of about 16 mA to a final value of 130 mA. The relative humidity in the effluents followed the same trends as the fuel cell current: when the current decayed the relative humidity in both streams approached zero, and when the fuel cell current increased the relative humidity increased. The critical initial water content for sustained operation corresponds to "ignition" of the fuel cell. When the initial membrane water content is greater than the critical level, water production is sufficient to sustain the water content in the membrane. At lesser initial water contents the resistance to proton current is too great and evaporation of water from the membrane exceeds water production, thereby dehydrating the membrane and extinguishing the current.

Figure 6B shows an experiment where the initial water loading in the membrane was the same, but the external load

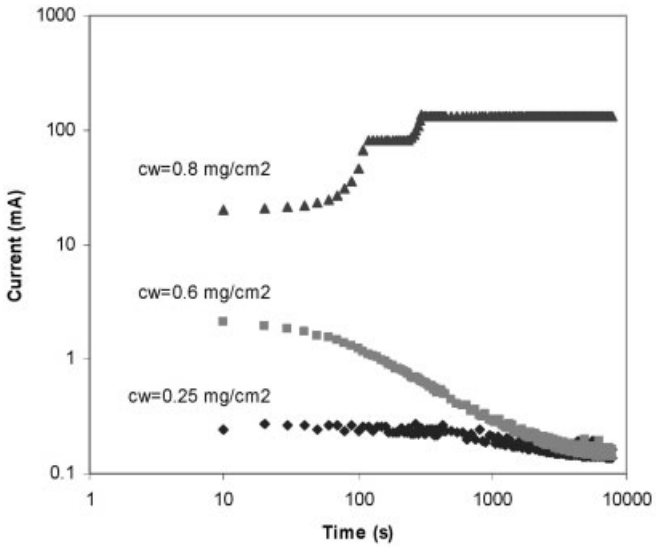

Figure 6a. STR PEM fuel cell startup from different initial membrane water contents.

The membrane was exposed to humidified nitrogen at room temperature to hydrate it, and then heated to 60°C, and a flow of 10 mL/min of H_2 to the anode and O_2 to the cathode was initiated.

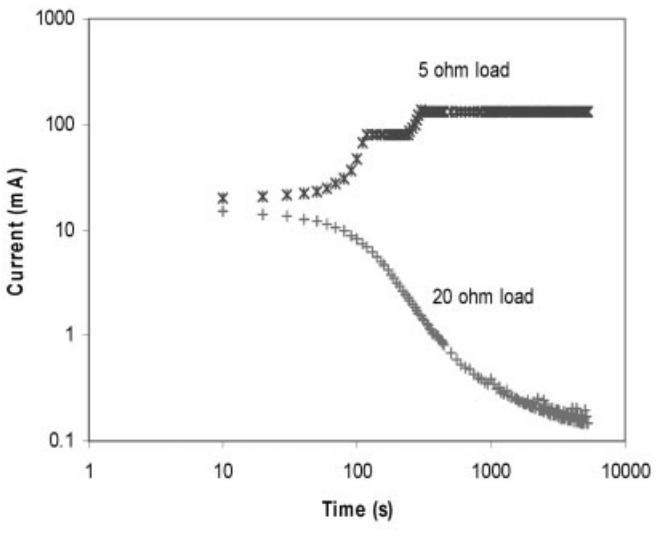

Figure 6b. STR PEM fuel cell startup with different load resistances.

The initial water content in both cases was about 0.8 mg/cm^2. The fuel cell was operated at 60°C and a flow of 10 mL/min of H_2 to the anode and O_2 to the cathode.

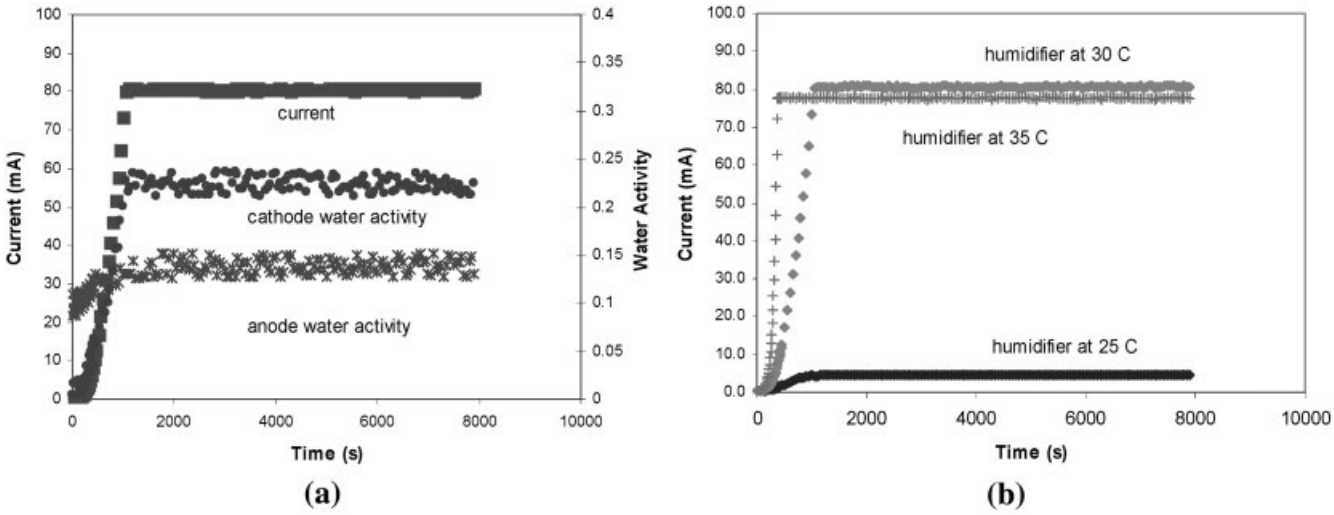

Figure 7. Startup of the STR PEM fuel cell operated at 60°C with feeds of 10 mL/min O_2 and 10 mL/min H_2.

(a) The membrane was initially dry. The hydrogen feed was humidified in a bubbler held at 30°C. The external load resistance was 7 Ω. (b) The membrane was initially dry. The hydrogen feed was humidified in a bubbler held at the temperatures shown in the figure. The external resistance was 7 Ω.

resistance was changed. The flow rates were still set to 10 mL/min for both H_2 and O_2 and the fuel cell temperature was 60°C. With an external load resistance of 5 Ω the fuel cell current ignited, increasing from about 20 mA to a final value of 150 mA. In contrast when the external load resistance was 20 Ω the current was extinguished, starting at about 7 mA and decaying. This result illustrates how the membrane and external load resistances act in series, and *either one* could limit the ultimate steady-state current.

Critical humidification of reactant feed

Humidifying the reactant feed may also result in ignition of the fuel cell. Figure 7A shows an experiment where the STR PEM fuel cell was initialized as described above with a "dry" membrane (the membrane was dried by flowing dry gases passing through the fuel cell at 60°C for 12 h). At time zero dry O_2 was introduced to the fuel cell at 10 cm^3/min, and 10 cm3/min H_2 feed was first passed through a bubbler. The bubbler temperature was controlled with an external heating tape connected to a Variac. Humidification of the anode feed "ignited" the fuel cell, as shown in Figure 7A. After ignition, the water produced further increases the water activity of the fuel cell effluents. The critical feed humidification for ignition is demonstrated in Figure 7B. Increasing the humidifier temperature from 25 to 30°C resulted in ignition of the fuel cell current. Further increase in the humidifier temperature to 35°C resulted in more rapid humidification of the membrane and earlier ignition of the fuel cell, although the final steady-state current was the same. The final steady-state current depends primarily on the water activity in the membrane, and only indirectly on the water content of the feed (as a threshold for ignition).

Ignition in the STR PEM fuel cell results from a positive feedback between water production and the reaction rate. As seen in Eq. 3 water production will alter the inventory of water in the membrane. The membrane resistance depends on the membrane water activity, as indicated by Eqs. 7 and 8. Increased membrane water activity decreases the membrane resistance, which according to Eq. 7 will increase the fuel cell current. The increased current produces more water that will further increase the water activity in the membrane. The current increase is self-limiting. At high membrane water activity liquid water condenses in the catalyst layer. The transport of oxygen to the catalyst/membrane interface through the water film is reduced relative to oxygen transport through a gas layer. By inhibiting the supply of oxygen to the cathode, water condensation limits the reaction rate (current). This corresponds to a shift in the rate-limiting step of the fuel cell reaction. When the water activity is low, proton transport across the membrane is rate limiting; when the water activity is unity, reactant transport from the gas to the cathode catalyst surface becomes rate limiting.

The ignition phenomenon reported here shows a direct analogy to thermal ignition for exothermic reactions in stirred tank reactors. With the autothermal reactor there is a critical initial temperature for ignition. The reactor can also be ignited by preheating the reactor feed (Folger, 1999; Froment and Bischoff, 1979; Liljenroth, 1918; van Heerden, 1953).

Fuel cell response to changes in load

When used for automotive applications, fuel cells need to respond to changes in the load. Changing the load alters the water production, changing the balance between water produced and water removed, resulting in a change in the membrane water content. The effect of the load resistance on the water activity can be seen in the polarization curves for the STR PEM fuel cell shown in Figure 8A. The STR PEM fuel cell was operated in the autohumidification mode. The STR PEM fuel cell was equilibrated at 80°C for 12 h with a fixed load resistance (either 0.2 or 20 Ω). After equilibration the polarization curve was obtained by sweeping the load resistance between 0.2 and 20 Ω in 100 s. The relative humidity in the anode and cathode streams changed by $<2\%$ while obtaining these polarization curves; for all practical purposes these

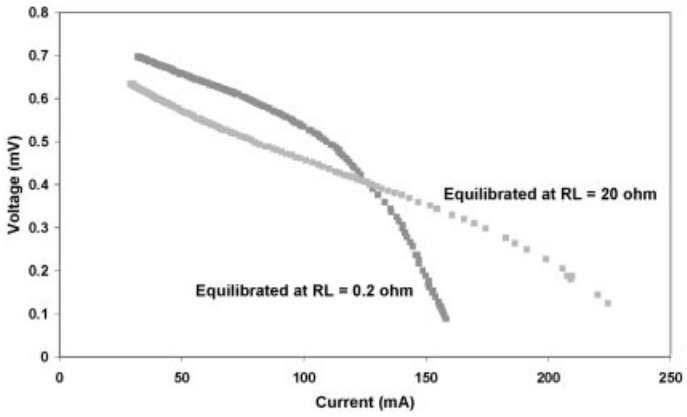

Figure 8a. "Instantaneous" polarization curves for STR PEM fuel cell equilibrated with a fixed load resistance at 80°C for 12 h.

The *IV* curves were recorded by sweeping the load resistance from 0 to 20 Ω in a period of 100 s.

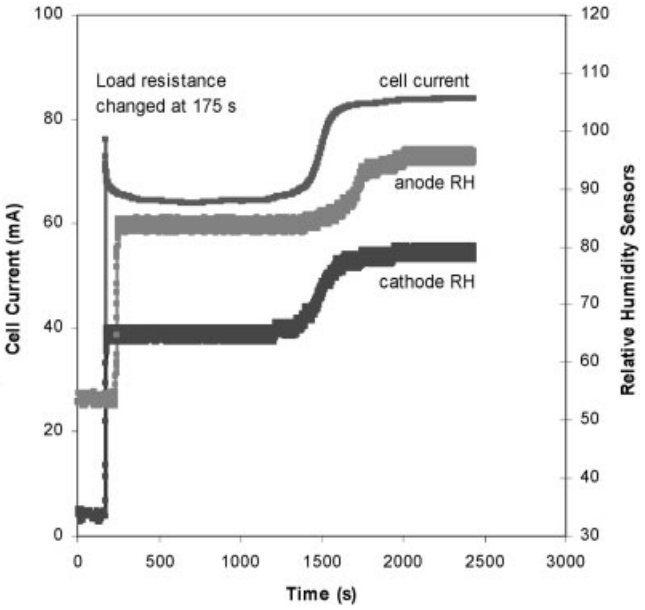

Figure 8b. Dynamic response of the STR PEM fuel cell for switching the load resistance from 20 to 7 Ω at 80°C.

The flow rates were 5 mL/min H_2 and 10 mL/min O_2. The resistance was switched at 175 s.

polarization curves are taken at "constant" membrane water activity.

Figure 8a illustrates that the "instantaneous" polarization curve does not represent a unique characterization of the PEM fuel cell. Operation with different load resistances for extended periods of time resulted in different membrane water activities. The membrane water activity is critical in defining the "instantaneous" polarization curve. The striking feature about Figure 8A is that the two polarization curves cross. Extended operation with a low load resistance produced an MEA with "high" water content, whereas extended operation with a high load resistance produces an MEA with "low" water content. The MEA with the high water content shows a higher voltage at low currents, indicating a lower activation polarization. At high currents the "high" water content of the MEA shows a lower voltage, suggesting the water is limiting mass transport of oxygen to the cathode. The "low" water content MEA has greater activation polarization, but a lower mass transport resistance.

The dynamic response of the STR PEM fuel cell to a change in resistive load shows an unusual multistep process. Figure 8b shows an immediate step response of the current to the change in load, followed by decay to plateau value. There was a subsequent jump in the fuel cell current after 1500 s. The time constant for the increase to the initial plateau was about 10 s. There was a delay of about 100 s in the change of the water activity at the anode relative to the change in current and the change in water activity at the cathode. The jump in current after 1500 s occurred with no changes to any external parameter and was completely unexpected. The cathode relative humidity response tracks the current response; the anode relative humidity response tracked the current but was delayed by about 100 s.

The response times of a PEM fuel cell may be considered surprising. It does not fit with the common assumption that PEM fuel cells have response times of milliseconds, which make them appropriate for use in automobiles. The data show at least four different time constants associated with the dynamic response of the fuel cell to changes in load. The initial response that occurs almost instantaneously must correspond to the change in current at constant membrane water content. The other time constants must correspond to transport processes, and changes in the membrane properties that result from changes in membrane water content.

What physical processes can account for the PEM fuel cell responses?

We can compare various time constants associated with the PEM fuel cell. Four of the key time constants are listed in Table 2. They include: the characteristic reaction time of the PEM fuel cell (τ_1), the time for gas phase transport across the diffusion layer to the membrane electrode interface (τ_2), the characteristic time for water to diffuse across the membrane from the cathode to the anode (τ_3), and the characteristic time for water produced to be absorbed by the membrane (τ_4). Approximate values for the physical parameters were used to obtain order-of-magnitude estimates of these time constants. The estimated time constants shown in Table 2 indicate that the response times of about 100 s are associated with water uptake and transport through the membrane.

The 100-s time for water transport through the membrane is evident in the delay of the response of the water activity in the anode effluent compared to the increase in current. Water absorption by the membrane has a time constant of about 10–100 s. Operating at a current density of 1 A/cm^2 it would take about 100 s to saturate a dry membrane with water (assuming no water evaporates into the gas effluents from the

Table 2. Characteristics Times for PEM Fuel Cells

Time	Physical Significance		Approximate Value (s)
τ_1	Characteristic time for reaction rate relative to reactor volume	$\tau_1 = \frac{V_R}{i} \sim \frac{(0.1\ \text{cm}^3/\text{cm}^2)}{(1\ \text{A/cm}^2)}$	0.1
τ_2	Characteristic diffusion time across gas diffusion layer	$\tau_2 = \frac{(\ell_{diffusion\ layer})^2}{(D_{gas}^{eff})} \sim \frac{(0.03\ \text{cm})^2}{(0.01\ \text{cm}^2/\text{s})}$	0.1
τ_3	Characteristic diffusion time for water across membrane from cathode to anode	$\tau_3 = \frac{(\ell_{membrane})^2}{(D_{water}^{membrane})} \sim \frac{(0.01\ \text{cm})^2}{(10^{-6}\ \text{cm}^2/\text{s})}$	100
τ_4	Characteristic time for water production relative to sulfonic acid density	$\tau_4 = \frac{\lambda N_{SO3}}{i} \sim \frac{5(2.3 \times 10^{-5}\ \text{mol/cm}^2)}{(1\ \text{A/cm}^2)}$	100

fuel cell). Likewise when the load resistance is increased, the finite evaporation rate results in a slow decay to steady state. The membrane acts as a reservoir for water as the external load resistance, reactant flow rates, and temperature changes alter the balance between water production and water removal. The dynamic model presented in Figure 4 includes an essential element missing from most PEM fuel cell models in the literature. Equation 3 is the mass balance of water in the membrane, and Eqs. 6–8 relate the change in the reaction rate (fuel cell current) to the changes in the water content in the membrane. The dynamics of PEM fuel cell operation are critically dependent on the water balance in the membrane, which is evident in all our experimental results presented here.

The 1500-s time constant for the second jump in the current shown in Figure 8B is still not well understood. We recently measured the stress relaxation of Nafion. A Nafion 117 sample was strained to 50%, beyond its yield point for plastic deformation, and the stress was measured as a function of time. At room temperature the stress took about 4000 s to relax to a constant value. We believe the jump in the current after 1500 s is attributable to the relaxation of the stress in the membrane. Increased membrane water content results in the membrane swelling, which puts the membrane under stress. Relaxation of the membrane stress appears to reduce the electrical resistance of the membrane.

Response to temperature changes

The dynamic response of the fuel cell to changes in the temperature can be used to explore the dynamic response of fuel cells to changes in heat dissipated. The response of the STR PEM fuel cell to a change in temperature is shown in Figures 9A and 9B. The fuel cell was operated with fixed feed flow rates of 10 mL/min H_2 at the anode and 10 mL/min O_2 at the cathode. The load resistance was fixed at 2 Ω. After changing the setpoint on the temperature controller, the temperature, cell current and voltage, and the relative humidity in the anode and cathode effluents were monitored. The temperature controller could actively heat the cell from 70 to 90°C in about 200 s; cooling was passive, so it took about 1400 s for the temperature to fall from 90 to 70°C. As the temperature fell, the current and effluent relative humidities all increased. The decrease in the water vapor pressure with temperature reduced the rate of water removal. With less water removed, the water activity in the membrane increased, resulting in a higher current. The relative humidity in the effluents also increased,

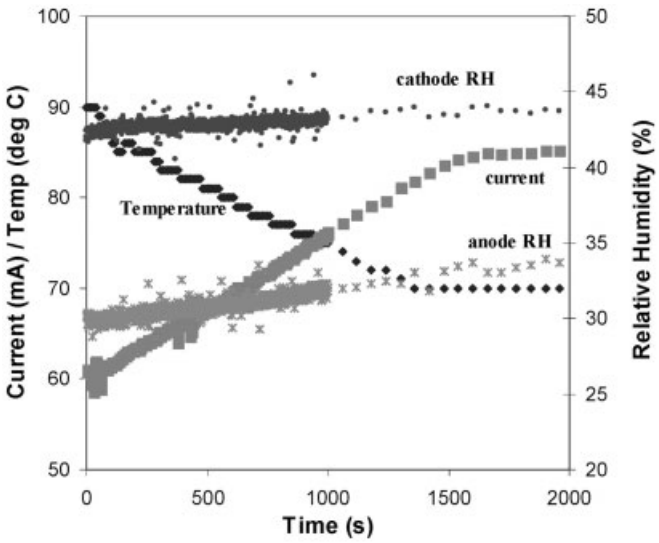

Figure 9a. STR PEM fuel cell response to a decrease in temperature from 90 to 70°C.

H_2 flow and O_2 flow were both 10 mL/min and the external load resistance was 2 Ω.

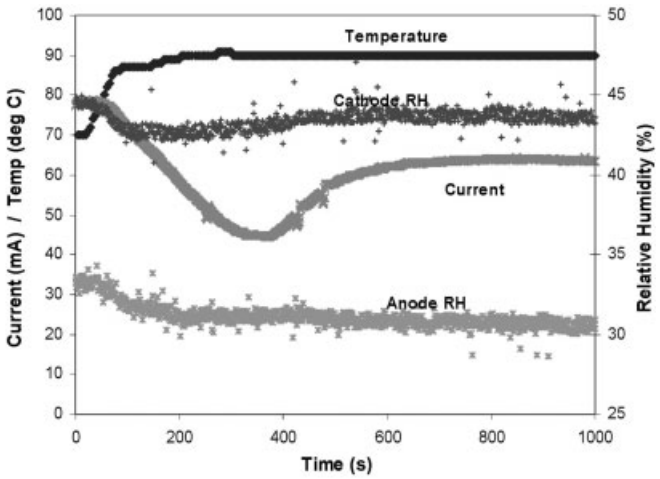

Figure 9b. STR PEM fuel cell response to an increase in temperature from 70 to 90°C.

H_2 flow and O_2 flow were both 10 mL/min and the external load resistance was 2 Ω.

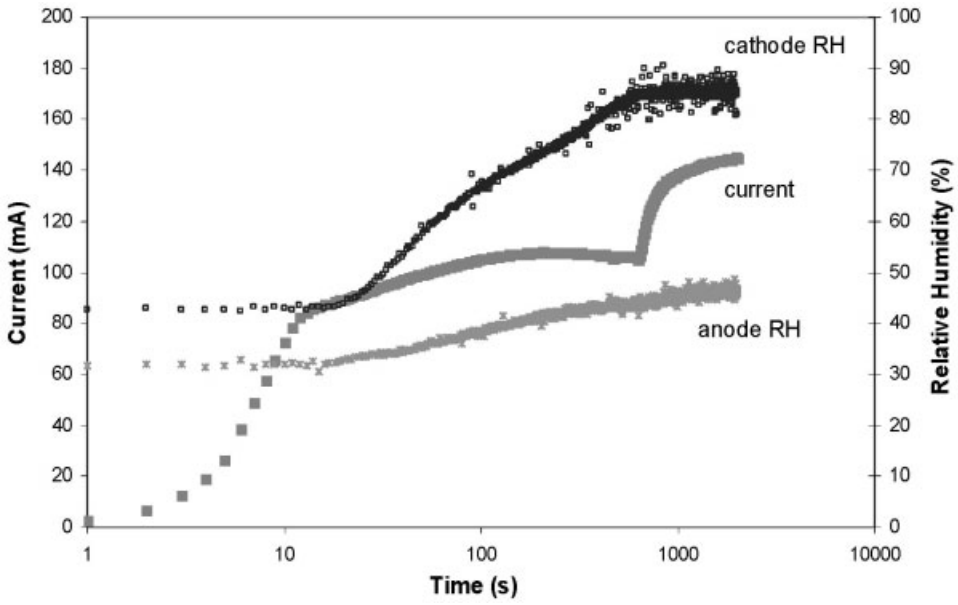

Figure 10. Response of the STR PEM fuel cell to a change in anode flow rate.

The H_2 feed to the anode was increased from 1 mL/min to 10 mL/min at time 0. The O_2 feed to the cathode was constant at 10 mL/min, the cell temperature was 80°C, and the load resistance was 2 Ω.

because the vapor pressure of water is lower, so even for the same partial pressure of water in the effluent streams the relative humidity is greater.

The response of the STR PEM fuel cell to an increase in temperature was surprising. The current and relative humidity in both effluent streams initially decreased. The current and cathode relative humidity went through minima before approaching the steady state. This suggests that evaporation from the MEA is faster initially than the diffusion of water across the membrane. It took the current and relative humidity over 700 s to reach steady state, whereas the temperature was at steady state after only 200 s. The long transition to steady state resulted from equilibration between water in the membrane and water at the membrane–electrode interfaces. The differences in the relative humidity responses at the anode and cathode are indicative of the complex coupling between water transport into and through the membrane and water production at the cathode.

Raising the temperature increased the water vapor pressure, which increases the water removal rate from the fuel cell. At constant water activity the membrane resistance has a weak temperature dependency (Yang, 2003). Increasing the temperature from 80 to 140°C decreases the resistivity of Nafion by 50%. The water vapor pressure increased by about 700% over the same temperature span. With all else the same, the higher temperature will reduce the water content in the membrane and ultimately reduce the current.

Response to changes in reactant flow rates

The flow rates to the anode of the fuel cell should be varied during operation to achieve high hydrogen utilization. The dynamic response of the STR PEM fuel cell to changes in H_2 flow is shown in Figure 10. The STR PEM fuel cell was equilibrated for 12 h with a H_2 flow of 1 mL/min and then the H_2 flow was rapidly increased to 10 mL/min. The oxygen flow to the cathode was kept constant at 10 mL/min. The cell temperature was 80°C and the external load resistance was 2 Ω. The cell current rapidly increased from 3 to about 80 mA during the first 10 s after the change in flow rate. The current increased more slowly over the next 100 s and leveled off at about 100 mA. The relative humidity at the cathode began to increase 10 s after the flow rate was increased and the current increased. The cathode relative humidity continued to climb steadily as the current leveled off. The current jumped suddenly after about 650 s from 105 to 145 mA, and the relative humidity at the cathode increased much more slowly after 650 s. The anode relative humidity showed a steady increase for the entire 2000 s of the test run.

The dynamic response during the first 650 s, shown in Figure 10, was expected. Increasing the supply of hydrogen increased current and water production. With more water produced, more water exited through the effluent streams because of increased relative humidity. The jump in the current after 650 s is surprising. We believe the jump in current results from water swelling the membrane and mechanical stress relaxation improving the membrane–electrode contact. We have observed this phenomenon in other contexts of PEM fuel cell dynamics and it is the subject of ongoing investigations.

"Stationary state" operation

The dynamic data presented so far were all in response to changes in system parameters. We chose to present "well-behaved" responses, so that the behavior could be easily rationalized. Dynamic data for the STR PEM fuel cell can be much more complex than what we presented here. We conclude with

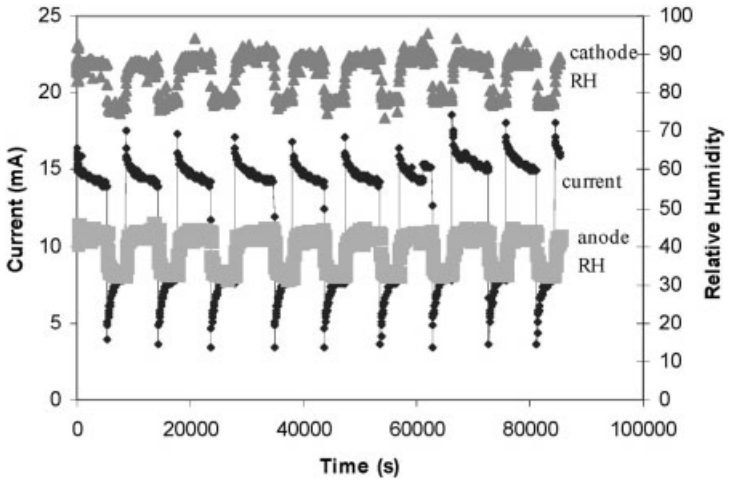

Figure 11. Stationary-state response of STR PEM fuel cell over a 24 h period.

The feed flow rates were 5 mL/min of H_2 and 10 mL/min O_2, the cell temperature was 80°C, and the load resistance was 20 Ω.

an example that illustrates some of the complex dynamics of the STR PEM fuel cell that are still far from being understood.

Figure 11 shows the stationary-state response of the STR PEM fuel cell over a 24 h period. All the external controllable parameters were fixed. The feed flow rates were constant at 5 mL/min of H_2 to the anode and 10 mL/min O_2 to the cathode. The fuel cell temperature was fixed at 80°C and the load resistance was fixed at 20 Ω. The current, voltage, and relative humidity in the effluent streams all displayed autonomous oscillations with a frequency of 10^{-4} Hz! The current oscillations were large in amplitude, changing by a factor of 2 between 75 and 170 mA. The current oscillations overshot and undershot the plateau values at the high and low states. The effluent relative humidity at both the anode and cathode oscillated in phase with the current.

We observed these autonomous oscillations under a variety of conditions of temperature, flow rate, and load resistance. We believe the oscillations are caused by coupling between the mechanical relaxation of the polymer membrane to changes in the water content and the membrane electrode interfacial resistance. However, we are still a long way from understanding the physics in sufficient detail to develop predictive dynamic models for these results. Complex dynamic behavior has been anecdotally reported for fuel cell test stations, but seems to have been ignored because of lack of models that predict any such behavior. The STR PEM fuel cell displays the oscillations distinctly, and we believe that, by uncoupling the temporal oscillations from spatial variations, we can clarify their origin and control them. Data of this quality and relative simplicity shown here are essential to understand the complex dynamics of PEM fuel cells.

Conclusions

Our purpose herein was to introduce the use of a differential reactor to study fuel cell dynamics. The data presented here show that the PEM fuel cell responses are characterized by time constants varying from less than a second to thousands of seconds. The STR PEM fuel cell is a one-dimensional differential reactor that is ideally suited to examine dynamics of the coupling of reaction and transport processes in a polymer membrane fuel cell. The STR PEM has even unveiled novel behavior that suggests mechanical properties of the polymer membranes may play an important role in fuel cell dynamics.

The STR PEM fuel cell is not *an optimal design of a fuel cell reactor*, in the sense of obtaining the highest power output or highest fuel efficiency. Its purpose is to provide a well-defined set of reactor conditions to facilitate the correlation of fuel cell operation with process parameters. We have stressed the importance of characterizing the system variables and relating them to changes in the system parameters. This approach is vital to the development of effective control systems for fuel cells.

The STR PEM fuel cell has exemplified how PEM fuel cells "ignite" and the critical role the water balance plays in the dynamics of ignition. The water activity in the membrane must equilibrate with changes in the control parameters, feed flow rates, cell temperature, and load resistance. Changes in the control parameters alter the balance between water production and water removal. PEM fuel cells typically have at least two time constants associated with their transient responses. There is a very rapid response, time constant < 1 s, corresponding to the changes in external load at constant membrane water activity. There are longer responses, with time constants of about 100 s, corresponding to water transport in the membrane and equilibration of the membrane water activity. Finally we showed there are additional dynamic processes with time constants of about 1000–10,000 s, probably attributable to mechanical relaxation processes that are not yet fully understood.

Acknowledgments

The authors thank the Air Force Office of Scientific Research (AFOSR, Dynamics and Control Grant F 49620-03-1-0097) and the National Science Foundation (NSF Grant CTS-0354279, NSF ITR Grant CTS-025484, and NSF REU Grant DMR-0139107) for support of this research.

Notation

A_m = area of membrane
a_w^i = water activity at anode (A), cathode (C), or membrane (m)
EW = equivalent weight of membrane, mass/mole of SO_3

F = Faraday's constant
ΔG° = free energy of the fuel cell reaction
i = current
N_w^m = water content in membrane, moles
P_i = partial pressure of species i, bar
Q_i = volumetric flow rate
R = gas constant
R_m = effective resistance of the membrane electrode assembly
R_L = external load resistance
T = fuel cell temperature
V_{eff} = effective output voltage of fuel cell
V_i = gas volume at anode (A) and cathode (C)
Δz = membrane thickness
η = overpotential of fuel cell (a function of membrane water activity and load resistance)
λ_w = absorbed water concentration per sulfonic acid content, # water/# SO_3

Literature Cited

Baschuk, J. J., and X. H. Li, "Modeling of Polymer Electrolyte Membrane Fuel Cells with Variable Degrees of Water Flooding," *J. Power Sources*, **86**, 181 (2000).

Bernardi, D. M., "Water-Balance Calculations for Solid-Polymer-Electrolyte Fuel Cells," *J. Electrochem. Soc.*, **137**, 3344 (1990).

Bernardi, D. M., and M. W. Verbrugge, "A Mathematical-Model of the Solid-Polymer-Electrolyte Fuel Cell," *J. Electrochem. Soc.*, **139**, 2477 (1992).

Blomen, L. J. M. J., and M. N. Mugerwa, eds., *Fuel Cell Systems*, Plenum, New York (1993).

Bokris, J. O. M., and S. Srinivasan, *Fuel Cells: Their Electrochemistry*, McGraw-Hill, New York (1969).

Costamagna, P., and S. Srinivasan, "Quantum Jumps in the PEMFC Science and Technology from the 1960s to the Year 2000. Part II. Engineering, Technology Development and Application Aspects," *J. Power Sources*, **102**, 253 (2001).

Dutta, S., S. Shimpalee, and J. W. Van Zee, "Three-Dimensional Numerical Simulation of Straight Channel PEM Fuel Cells," *J. Appl. Electrochem.*, **30**, 135 (2000).

EG&G Services, *Fuel Cell Handbook*, US Department of Energy, Morgantown, WV (2000).

Folger, H. S., *Elements of Chemical Reaction Engineering*, Prentice Hall, Upper Saddle River, NJ (1999).

Froment, G. F., and K. B. Bischoff, *Chemical Reactor Analysis and Design*, Wiley, New York (1979).

Levenspiel, O., *The Chemical Reactor Omnibook*, OSU Book Stores, Corvallis, OR (1996).

Liljenroth, F. G., "Starting and Stability Phenomena of Ammonia-Oxidation and Similar Reactions," *Chem. Metall. Eng.*, **19**, 287 (1918)

Natarajan, D., and T. Van Nguyen, "A Two-Dimensional, Two-Phase, Multicomponent, Transient Model for the Cathode of a Proton Exchange Membrane Fuel Cell Using Conventional Gas Distributors," *J. Electrochem. Soc.*, **148**, A1324 (2001).

Raistrick, I. D., "Electrode Assembly for Use in a Solid Polymer Electrolyte Fuel Cell," U.S. Patent No. 4 876 115 (1989).

Springer, T. E., T. Rockward, T. A. Zawodzinski, and S. Gottesfeld, "Model for Polymer Electrolyte Fuel Cell Operation on Reformate Feed—Effects of CO, H_2 Dilution, and High Fuel Utilization," *J. Electrochem. Soc.*, **148**, A11 (2001).

Springer, T. E., T. A. Zawodzinski, and S. Gottesfeld, "Polymer Electrolyte Fuel-Cell Model," *J. Electrochem. Soc.*, **138**, 2334 (1991).

Thampan, T., S. Malhotra, H. Tang, and R. Datta, "Modeling of Conductive Transport in Proton-Exchange Membranes for Fuel Cells," *J. Electrochem. Soc.*, **147**, 3242 (2000).

Thampan, T., S. Malhotra, J. X. Zhang, and R. Datta, "PEM Fuel Cell as a Membrane Reactor," *Catalysis Today*, **67**, 15 (2001).

van Heerden, C., "Autothermic Processes: Properties and Reactor Design," *Ind. Eng. Chem.*, **45**, 1242 (1953).

Van Nguyen, T., and M. W. Knobbe, "A Liquid Water Management Strategy for PEM Fuel Cell Stacks," *J. Power Sources*, **114**, 70 (2003).

Yang, C. R., "Performance of Nafion/Zirconium Phosphate Composite Membranes in PEM Fuel Cells," Department of Mechanical Engineering, Princeton University, Princeton, NJ (2003).

Manuscript received Oct. 6, 2003, and revision received Nov. 13, 2003.